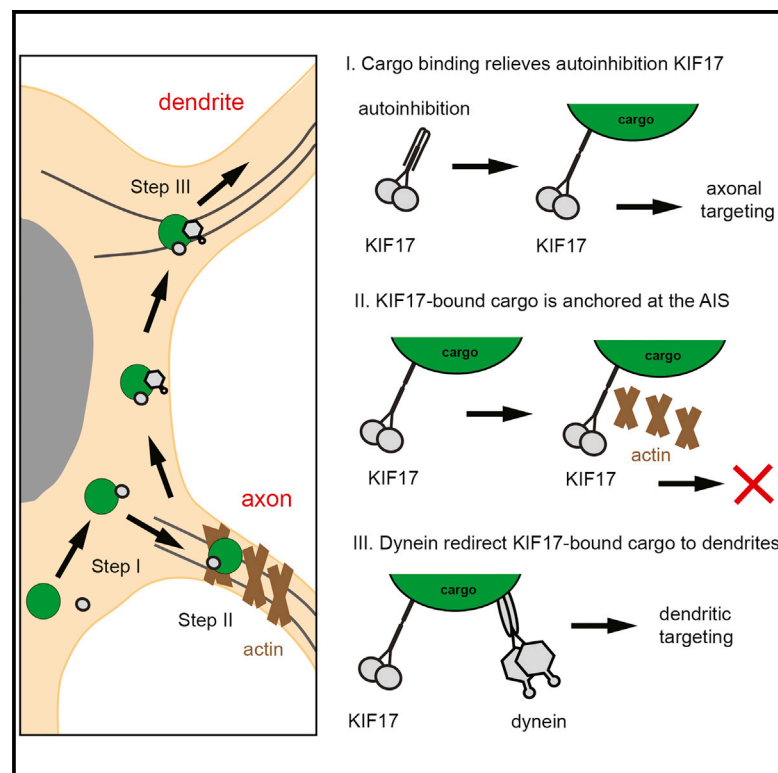


# Current Biology

## Three-Step Model for Polarized Sorting of KIF17 into Dendrites

### Graphical Abstract



### Authors

Mariella A. Franker,  
Marta Esteves da Silva,  
Roderick P. Tas, ..., Phebe S. Wulf,  
Lukas C. Kapitein,  
Casper C. Hoogenraad

### Correspondence

c.hoogenraad@uu.nl

### In Brief

In neurons, the kinesin-2 family protein KIF17 is a dendrite-specific motor protein and has been shown to interact with several dendritic cargoes. Franker et al. found that the polarized sorting of KIF17 to dendrites is regulated in three steps, in which dynein motor activity is required for proper dendritic sorting.

### Highlights

- Cargo binding relieves autoinhibition of KIF17 in living cells
- KIF17-bound cargo does not autonomously target dendrites
- KIF17-bound cargoes enter the axon but anchor at the AIS
- Dynein redirects KIF17-bound cargo into dendrites



# Three-Step Model for Polarized Sorting of KIF17 into Dendrites

Mariella A. Franker,<sup>1,2</sup> Marta Esteves da Silva,<sup>1,2</sup> Roderick P. Tas,<sup>1,2</sup> Elena Tortosa,<sup>1</sup> Yujie Cao,<sup>1</sup> Cátia P. Frias,<sup>1</sup> Anne F.J. Janssen,<sup>1</sup> Phebe S. Wulf,<sup>1</sup> Lukas C. Kapitein,<sup>1</sup> and Casper C. Hoogenraad<sup>1,\*</sup>

<sup>1</sup>Cell Biology, Department of Biology, Faculty of Science, Utrecht University, 3584 CH Utrecht, the Netherlands

<sup>2</sup>Co-first author

\*Correspondence: [c.hoogenraad@uu.nl](mailto:c.hoogenraad@uu.nl)

<http://dx.doi.org/10.1016/j.cub.2016.04.057>

## SUMMARY

Kinesin and dynein motors drive bidirectional cargo transport along microtubules and have a critical role in polarized cargo trafficking in neurons [1, 2]. The kinesin-2 family protein KIF17 is a dendrite-specific motor protein and has been shown to interact with several dendritic cargoes [3–7]. However, the mechanism underlying the dendritic targeting of KIF17 remains poorly understood [8–11]. Using live-cell imaging combined with inducible trafficking assays to directly probe KIF17 motor activity in living neurons, we found that the polarized sorting of KIF17 to dendrites is regulated in multiple steps. First, cargo binding of KIF17 relieves autoinhibition and initiates microtubule-based cargo transport. Second, KIF17 does not autonomously target dendrites, but enters the axon where the actin cytoskeleton at the axon initial segment (AIS) prevents KIF17 vesicles from moving further into the axon. Third, dynein-based motor activity is able to redirect KIF17-coupled cargoes into dendrites. We propose a three-step model for polarized targeting of KIF17, in which the collective function of multiple motor teams is required for proper dendritic sorting.

## RESULTS AND DISCUSSION

### Full-Length KIF17 Localizes to Dendrites, and Tailless KIF17 Targets the Axon

Consistent with previous findings [4, 5], we found that endogenous KIF17 and exogenously expressed full-length KIF17 (KIF17-FL) localized to the dendritic compartment (MAP2 positive) of mature hippocampal neurons in culture (Figures 1A–1E and S1A). Quantification revealed that endogenous KIF17 is localized to dendrites in developing (DIV6) and mature (DIV15) neurons; only ~5% of the cells show accumulations in axon tips, and no axon initial segment (AIS) (NF-186 positive) enrichment is observed (Figures 1A and 1F). Interestingly, overexpressed KIF17-FL targeted the axon (~85%) in young neurons (DIV6), whereas in more mature neurons (DIV15) the localization of KIF17-FL was largely dendritic (~10% of neurons with axonal

tip accumulation and no AIS accumulation) (Figures 1F, S1B, and S1C). As reported [8–11], a truncated form of KIF17 containing the motor domain and dimerization region (amino acids 1–547) but lacking the tail domain, hereafter referred to as KIF17-MD, targeted the axon and accumulated in axon tips in both young and mature neurons (~80% and ~90%, respectively; Figures 1E–1H). Together, these data demonstrate that the motor domain is selective for the axon and that the tail region regulates the dendritic targeting of KIF17 in mature neurons.

### Cargo Binding Relieves Autoinhibition of Full-Length KIF17

Autoinhibition is a well-described regulatory mechanism for kinesins in which the tail domain interacts with the motor domain and prevents motor activity [12–16]. It has been suggested that cargo binding may unfold autoinhibited motors to initiate microtubule-based transport. In vitro studies have shown that binding kinesin to beads activates the motor [17, 18]. Expression of KIF17-FL in COS7 cells showed a diffuse cytoplasmic pattern without any microtubule labeling (Figure 2A). In contrast, both the KIF17-MD and coiled-coil 2 (CC2) mutant KIF17-G754E, which has no autoinhibition [16], showed a strong microtubule staining in the periphery of the cell (Figure 2A) and displayed fast motility toward the microtubule plus ends (Figure 2B). The KIF17-G754E mutant showed very fast motility on microtubules, with an instantaneous speed of  $3.2 \pm 0.1 \mu\text{m/s}$  (Figure 2B). These data suggested that cargo-unbound KIF17-FL is autoinhibited in living cells.

To investigate whether cargo binding can directly activate the motor in cells, we chemically induced the binding of KIF17 to peroxisomes using the FRB-FKBP dimerization system (Figure 2C) [11, 19]. We expressed KIF17-GFP-FRB and PEX-RFP-FKBP in COS7 cells, and addition of rapalog during live-cell imaging induced KIF17 binding to the cargo [20]. As shown by maximum projections, time-coded color plots, and kymographs, rapalog treatment allowed KIF17-FL, KIF17-MD, and KIF17-G754E to efficiently transport peroxisomes from the cell center to the cell periphery (Figures 2D–2E and Movie S1). The data suggested that the cargo binding relieves autoinhibition of KIF17-FL. Interestingly, analysis of displacement curves (Figures 2F, 2G, and S2A–S2E) showed that the onset of motility of KIF17-FL is markedly slower ( $t_{1/2} = 10.6 \pm 3.0 \text{ min}$ ) compared to KIF17-G754E ( $t_{1/2} = 5.5 \pm 2.9 \text{ min}$ ) and KIF17-MD ( $t_{1/2} = 4.7 \pm 2.2 \text{ min}$ ). Next, we analyzed the speed of single peroxisomes (Figure 2H). Immobile peroxisomes were excluded from the analysis, and only minimum track

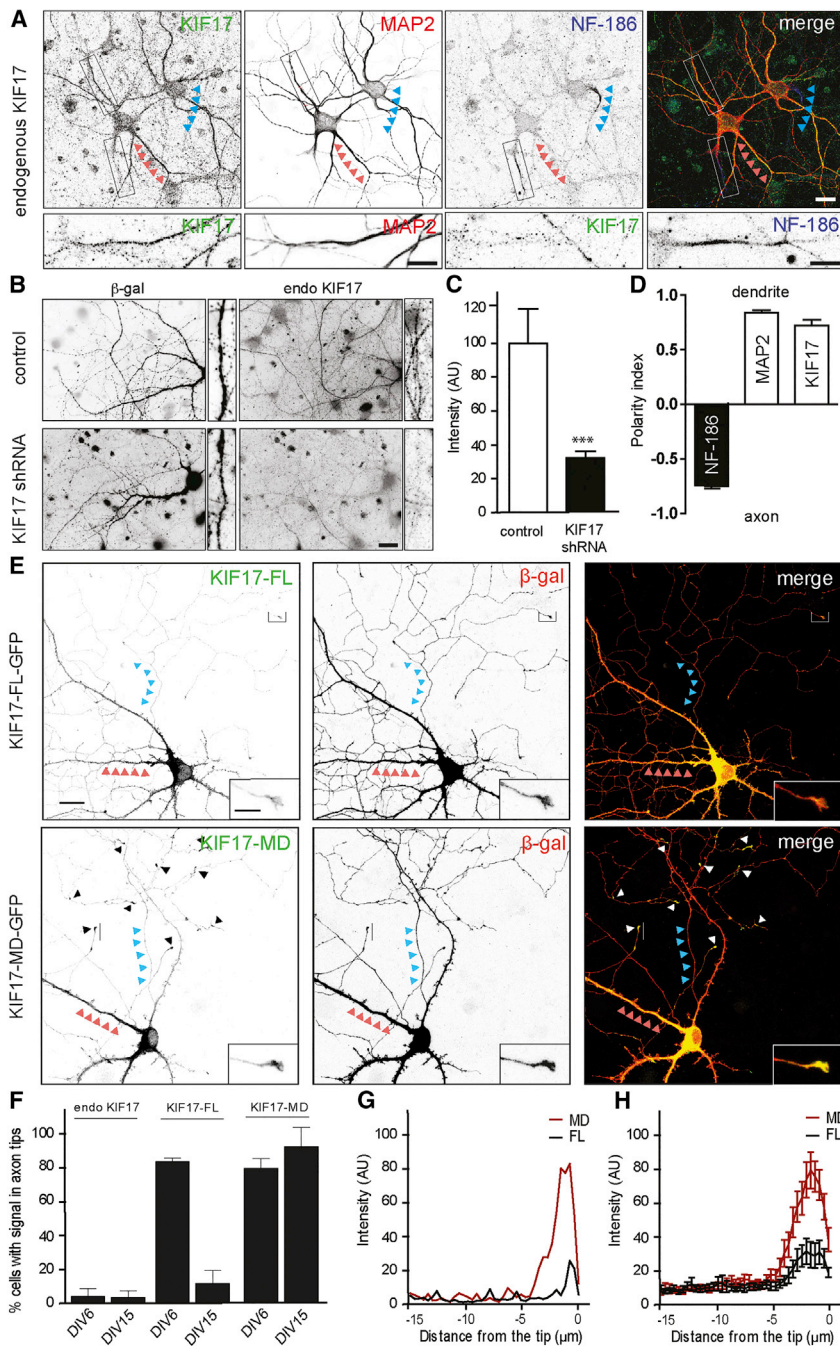


### Figure 1. Full-Length and Truncated KIF17 Constructs Localize to Different Neuronal Compartments

(A) Hippocampal neurons at DIV15 co-stained for endogenous KIF17, dendritic marker MAP2, and axon initial segment marker NF-186. (B) Hippocampal neurons at DIV11+3 co-transfected with pSuper control or KIF17 shRNAs and  $\beta$ -galactosidase ( $\beta$ -gal) to highlight neuronal morphology and stained for endogenous KIF17 and  $\beta$ -gal. (C) Quantification of KIF17 mean intensity in dendrites of neurons expressing pSuper control or KIF17 shRNAs (n = 34–38). (D) Polarity index of NF-186, MAP2, and KIF17 in DIV15 neurons (n = 12). (E) Hippocampal neurons at DIV19+2 co-transfected with  $\beta$ -gal and KIF17-FL-GFP or KIF17-MD-GFP. Inserts show zooms of axon tips. (F) Percentage of cells with accumulations in at least two axon tips in young (DIV6) and mature (DIV15) neurons with endogenous KIF17 and overexpressed KIF17-FL-GFP and KIF17-MD-GFP (n = 22–30). (G) Representative individual fluorescence intensity profile of KIF17-FL-GFP (black) and KIF17-MD-GFP (red) at the tip of the axon. (H) Average normalized fluorescence intensity profiles of KIF17-FL-GFP (n = 20) and KIF17-MD-GFP (n = 20) at the tip of the axon. Blue arrowheads indicate axons, and red arrowheads indicate dendrites. Scale bars, 20  $\mu$ m (A, B, and E), 10  $\mu$ m (A, insets), and 5  $\mu$ m (B and E, insets). Error bars indicate the SEM; \*\*\*p < 0.001 (Mann-Whitney test). See also Figure S1.

### Full-Length KIF17 Does Not Directly Target Dendrites but Is Anchored at AIS

To further study the role of the tail region on the dendritic targeting of KIF17, we used the cargo trafficking assay in cultured hippocampal neurons [11]. Without rapalog-induced motor coupling, the peroxisomes are largely immobile in hippocampal neurons (Figure S3A). After coupling KIF17 to peroxisomes, we observed that KIF17-FL was able to transport peroxisomes but did not target the dendrites. Instead, it had a strong preference for the axon, where the peroxisomes anchored at the AIS (Figures 3A–3C and Movie S2). In contrast, KIF17-

lengths of 1  $\mu$ m and 1 s were analyzed. All three KIF17 constructs showed similar single peroxisome behavior, with an average velocity around 1  $\mu$ m/s (mean  $\pm$  SD: FL = 1.07  $\pm$  0.50; MD = 0.91  $\pm$  0.47; G754E = 1.09  $\pm$  0.46  $\mu$ m/s) (Figure 2). These velocities were comparable to previous reports of kinesin-mediated organelle transport in cells (0.5–2  $\mu$ m/s) [4, 21]. These data indicate that the KIF17 motor domain alone and the non-autoinhibited KIF17 mutant quickly initiate cargo transport in living cells. These observations are consistent with the proposed role of the CC2 region in regulating KIF17 activity [16].

MD efficiently drove transport through the proximal axon. Earlier work established that the actin-rich AIS localized in the beginning of the axon functions as barrier for membrane-bound proteins [22], as well as transported cargoes [9, 23]. It was observed that dendritic cargoes halt and reverse in the AIS, suggesting that the AIS barrier prevents “unwanted” cargoes from entering the axon [24]. Furthermore, it has been shown that the actin cytoskeleton is important for the function of the AIS cytosolic barrier [9, 23, 24]. Next, we treated neurons with Latrunculin B (LatB) to depolymerize actin or expressed Ankyrin G (AnkG) short hairpin RNA (shRNA) to disrupt the AIS (Figures S1D and S1E) and

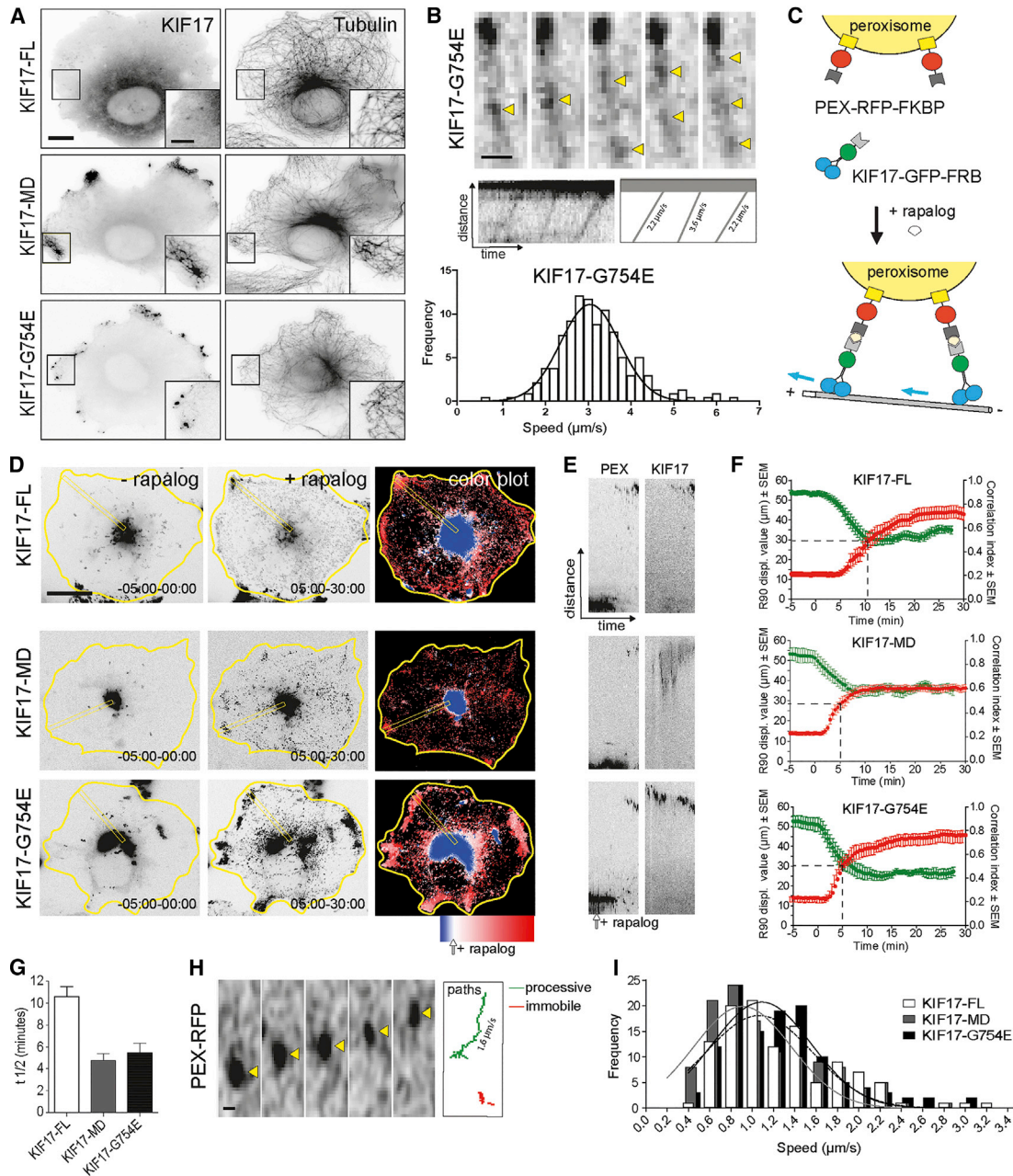


**Figure 2. Cargo Binding Activates Full-Length KIF17**

(A) COS7 cells transfected with KIF17-FL-GFP, KIF17-MD-GFP, or KIF17-G754E-GFP and stained with tubulin.

(B) Still frames and kymograph (3.2  $\mu\text{m} \times 5\text{ s}$ ) of KIF17-G754E-GFP moving toward the tip of a microtubule. The histogram of average speeds of KIF17-G754E-GFP ( $n = 31$  tracks) was fitted with a Gaussian function.

(C) Schematic representation of rapalog-induced coupling of KIF17-GFP-FRB to PEX-RFP-FKBP.

(D) Cargo transport efficiency of the indicated KIF17-GFP-FRB constructs. The left and middle panels show maximum projections of peroxisome motility before and after rapalog. The right panels are time-coded color plots.

(E) Kymographs (35  $\mu\text{m} \times 30\text{ min}$ ) of PEX-RFP-FKBP and KIF17-GFP as indicated in (D) (yellow boxes).

(F) Graphs showing R90 displacement value (red) and correlation index (green) of peroxisomes over time ( $n = 11-13$ ).

(G) Graph showing  $t_{1/2}$  of the indicated KIF17 constructs ( $n = 11-13$ ).

(H) Still frames of a single KIF17-FL-coupled peroxisome in COS7 cells at 10 frames per second (fps). The tracked paths of a processive and an immobile peroxisome are indicated.

(I) Histograms showing the average speeds of processive peroxisomes coupled to KIF17-FL, KIF17-MD, and KIF17-G754E ( $n = 113-121$  tracks) were fitted with a Gaussian fit.

Scale bars, 20  $\mu\text{m}$  (A and D), 5  $\mu\text{m}$  (A, inset), and 0.5  $\mu\text{m}$  (B and H). Error bars indicate the SEM. See also [Figure S2](#) and [Movie S1](#).

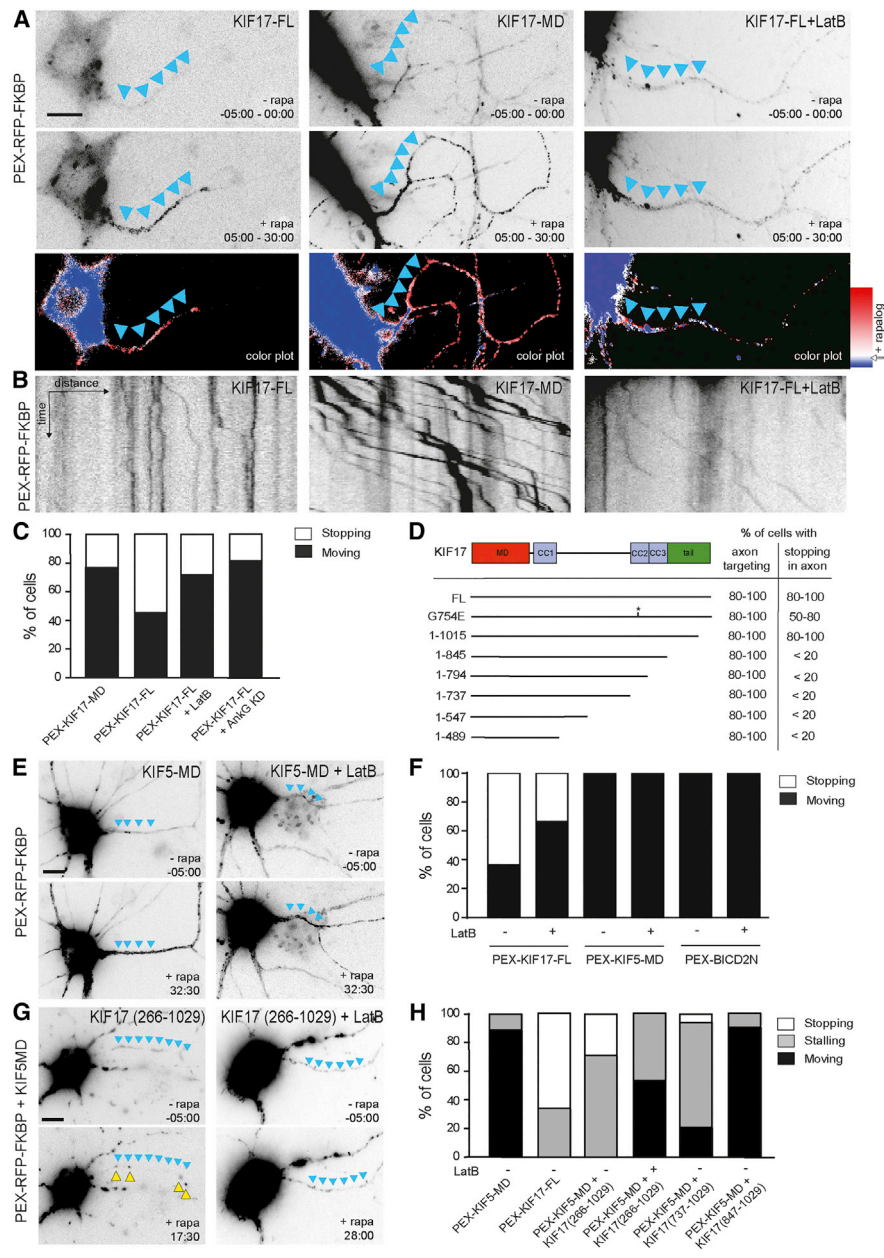


### Figure 3. The KIF17 Tail Region Mediates Cargo Stalling at the AIS

(A) Hippocampal neurons co-transfected with PEX-RFP-FKBP and KIF17-FL-GFP-FRB or KIF17-MD-GFP-FRB and live stained for the AIS marker Neurofascin. Cells expressing KIF17-FL were treated with 10  $\mu$ M Latrunculin B (LatB) for 1–2 hr before imaging. Maximum projections of peroxisome motility before and after rapalog addition (top) and color plots of peroxisome distributions (bottom) are shown.

(B) Kymographs (31  $\mu$ m  $\times$  31s) showing movement of peroxisomes in the proximal axon.

(C) Percentage of neurons with motile (moving) or non-motile (stopping) peroxisomes in the proximal axon expressing the indicated constructs (n = 11–16).

(D) Behavior of the various KIF17 constructs after peroxisome coupling characterized as percentage of cells with axon targeting and non-motile (stopping) peroxisomes in the proximal axon.

(E) Hippocampal neurons co-transfected with PEX-RFP-FKBP and KIF5-MD-GFP-FRB before and after rapalog addition, with and without LatB treatment. Images show maximum projections.

(F) Percentage of neurons with moving or stopping peroxisomes in the proximal axon after rapalog-induced coupling with KIF17-FL-GFP-FRB, KIF5-MD-GFP-FRB, or BICD2N-GFP-FRB, with and without LatB treatment (n = 11–16).

(G) Hippocampal neurons co-transfected with PEX-RFP-FKBP, KIF5-MD-GFP-FRB, and KIF17(266-1029)-GFP-FRB before and after rapalog addition, with and without LatB treatment.

(H) Percentage of neurons with moving, stalling, or stopping peroxisomes in the proximal axon after rapalog-induced coupling of KIF5-MD-GFP-FRB together with the indicated KIF17 constructs (n = 12–30).

Scale bars, 10  $\mu$ m (A, E, and G). See also [Figure S3](#) and [Movies S2](#) and [S3](#).

analyzed the behavior of KIF17-FL-coupled peroxisomes. We observed that disruption of the actin cytoskeleton or the AIS increased cargo motility and allowed axon transport comparable to KIF17-MD (Figure 3C and Movie S3). These data support the existence of an actin-based barrier at the AIS that regulates the entry of specific vesicles into the axon [9, 23]. Since LatB treatment did not affect KIF5- or dynein-coupled peroxisome motility (Figures 3E and 3F), the actin cytoskeleton is responsible for the specific KIF17-FL-coupled cargo accumulations in the AIS. Next, we generated several truncated KIF17 constructs and found that the tail region (amino acids 846–1015) was required for anchoring at the AIS (Figure 3D). Consistently, the shortest KIF17 construct that anchored at the AIS—KIF17(1–1015)—did not strongly accumulate in axonal tips (Figure S2). Interestingly, rapalog-induced coupling of both truncated KIF5 motors (KIF5-MD-GFP-FRB) and the KIF17-tail region (KIF17(266–1029)-GFP-FRB) to peroxisomes induced cargo stalling in the proximal axon (Figures 3G and 3H). Moreover, the KIF17-tail region also stalls KIF5-MD-induced Rab3-positive vesicles at the AIS, which can be suppressed by actin depolymerization (Figures S3B–S3E). Furthermore, expression of the KIF17-tail region (as a dominant-negative approach, without coupling to cargo) suppresses KIF17-FL-GFP-induced Rab3 stalling at the AIS (Figures S3F and S3G). These results indicate that the tail region of KIF17 is responsible for AIS anchoring.

One other possibility is that deactivation of KIF17 motor activity by back folding may cause cargo stalling at the AIS. However, our data argue against this option: KIF17-G754E shows strong axonal tip accumulation when overexpressed in neurons but still anchors at the AIS (Figures 3D and S2). However, local deactivation of KIF17 may still be achieved via additional mechanisms, such as inhibition of microtubule binding or ATP hydrolysis of the kinesin motor via local activation of regulatory protein in the AIS.

### KIF17 Vesicles Are Redirected into Dendrites by Cytoplasmic Dynein

Next we examined how KIF17 vesicles transported out of the proximal axon and into the dendrites and tested whether other motors present on the same cargo could redirect KIF17 transport. We first determined whether the retrograde motor dynein via recruitment of dynein adaptor BICD2 drives KIF17-bound vesicles out of the axon toward the soma. We expressed KIF17-FL-GFP-FRB, HA-BICD2N-FRB, and PEX-RFP-FKBP in neurons. Addition of rapalog recruited both KIF17-FL and BICD2N to peroxisomes and increased retrograde movement of peroxisomes in the proximal axon (Figures 4A–4C) from ~20% in neurons with KIF17-FL alone to ~50% in cells with KIF17-FL and BICD2N (Figure 4G). We next determined whether dynein also redirects KIF17-bound vesicles into dendrites. Addition of rapalog simultaneously recruited KIF17-FL and BICD2N to peroxisomes and quickly redistributed cargoes from the soma into the dendrites (Figures 4D–4F and Movie S4 and S5). Under these conditions, all neurons showed dendrite localization of KIF17-FL, whereas in the absence of BICD2N dendrite targeting is rare (Figure 4H). These results demonstrate that KIF17 vesicles can be redirected into dendrites by dynein motor activity.

Previous studies have analyzed the movements of KIF17-bound vesicles in neurons and therefore concluded that KIF17

actively transports cargoes into dendrites [3, 4]. Since various motor types (dynein, kinesin, and myosin) can simultaneously bind to cargo, it is challenging to interpret endogenous vesicle motility in neurons. This is particularly true in dendrites, where the microtubule cytoskeleton has opposite polarity orientations [25]. Moreover, motors attached to cargo can exist in active and inactive states and many regulators can influence their local motor activity [26]. By directly probing KIF17-mediated cargo movements, we found that full-length KIF17 does not target dendrites, but rather steers cargo into the axon, where it anchors at the AIS. We also demonstrate that dynein can drive KIF17-bound vesicles out of the axon and redirect them into the dendrites. These data fit well with the basic model for polarized transport in which most kinesins are responsible for transport into axons and dynein motors are responsible for transport into dendrites [1, 2]. Thus, the dendrite-specific localization of KIF17 is not due to active KIF17 transport from the soma to the dendrite, but to decreased axonal entry and the use of dynein activity to target dendrites. What is the role of KIF17 in dendrite-specific cargo trafficking? First of all, in contrast to many other kinesin family members, KIF17 is a unique plus-end-directed motor that prevents cargoes from entering the axon by AIS anchoring. The decreased axonal targeting emphasizes the importance of the actin-rich AIS in preventing “unwanted” cargoes from entering the axon and setting up the polarized distribution of somatodendritic proteins. Second, dynein helps to bring KIF17 into dendrites. However, once the more distal dendrites are reached, KIF17 may take over from dynein and deliver cargo toward the more distal dendritic regions. This idea is consistent with the observed motility of KIF17-bound cargoes within dendritic branches [11, 27]. Moreover, our data are in line with previous studies on polarized channel trafficking showing that KIF17 is required for K<sup>+</sup> channel Kv4.2 transport in dendrites but does not, by itself, specify dendritic localization of the channel [5]. However, additional studies are needed to determine whether the transport kinetics of KIF17-attached peroxisomes can be compared to a bona fide KIF17 cargo. Within dendrites, KIF17 may play a role in the spatial and temporal fine-tuning of receptor and/or channel trafficking to synapses [27–29]. Together, the data suggest that cooperativity between different motors is an important part of the polarized sorting mechanism. However, it remains an open question how coupling between KIF17 and dynein is regulated. Several studies have shown that interaction between different motor types occurs via adaptor proteins, which act as a “switch” between two motors to mediate trafficking [26, 30]. Future research will have to clarify how KIF17 and dynein interact with adaptors and which regulators are involved to achieve targeted trafficking.

## EXPERIMENTAL PROCEDURES

### Animals and Ethics Statement

All animal experiments were performed in compliance with the guidelines for the welfare of experimental animals issued by the federal government of the Netherlands. All animal experiments were approved by the Animal Ethical Review Committee (DEC) of Utrecht University.

### DNA Constructs, shRNA Sequences and Antibodies

The KIF17 expression constructs were generated by a PCR-based strategy using the human KIF17 cDNA (accession number NM\_020816; IMAGE clone

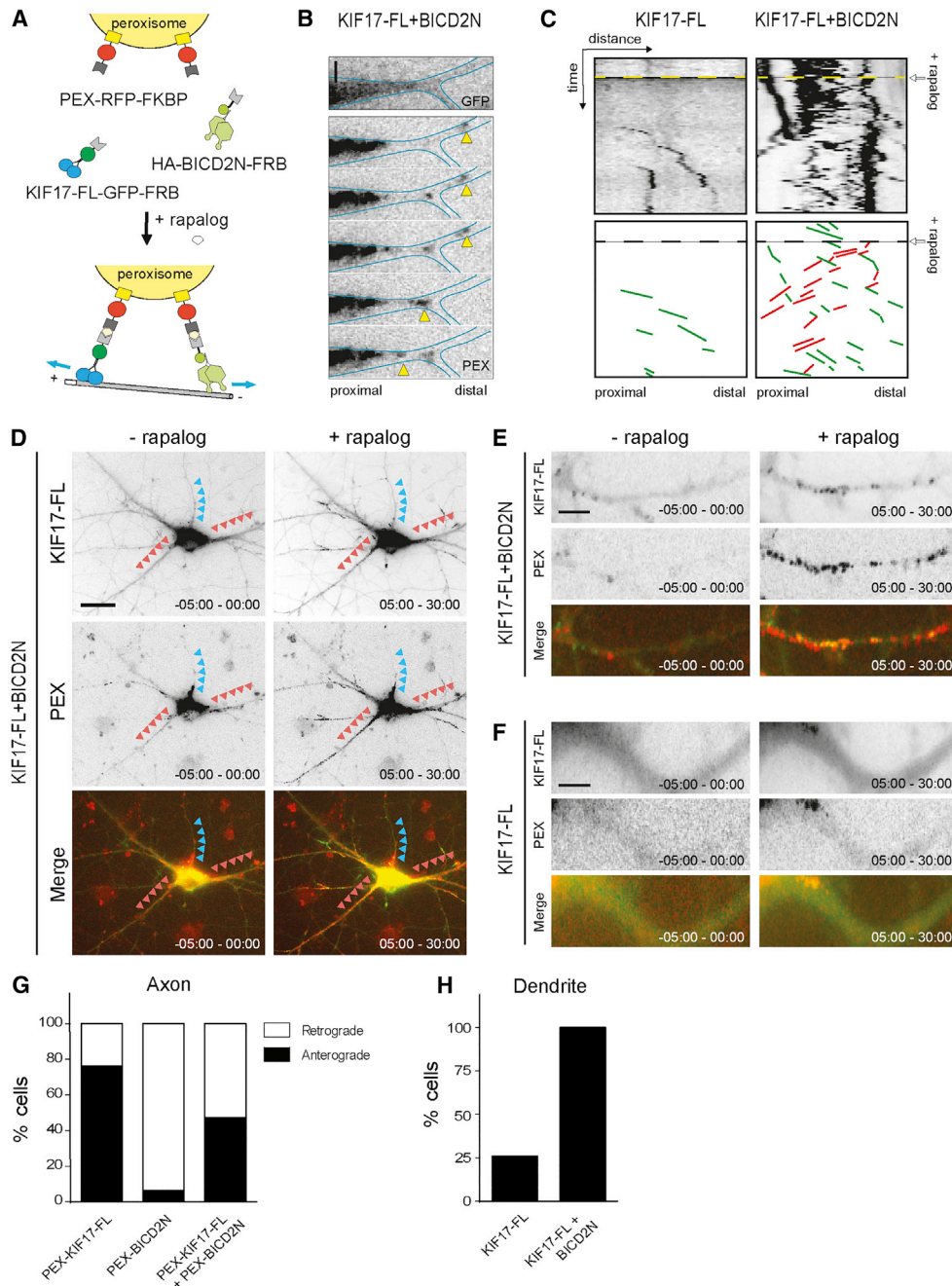


**Figure 4. Dynein Redirects KIF17 to Dendrites**

(A) Schematic representation of rapalog-induced co-coupling of KIF17-FL-GFP-FRB and dynein adaptor HA-BICD2N-FRB to PEX-RFP-FKBP.  
 (B) Still frames of retrograde peroxisome movement in the proximal axon at 30 s interval after simultaneous recruitment of HA-BICD2N-FRB and KIF17-FL-GFP-FRB.  
 (C) Kymographs (25  $\mu\text{m} \times 45 \text{ min}$ ) show increased retrograde movement of KIF17-FL-coupled peroxisomes in proximal axon in the presence of BICD2N-FRB. Illustrations of manually traced cargo displacements are indicated.  
 (D) Maximum projections of KIF17-FL-GFP and peroxisomes movements in neurons expressing PEX-RFP-FKBP, HA-BICD2N-FRB, and KIF17-FL-GFP-FRB before and after rapalog addition.  
 (E and F) Maximum projections before and after rapalog of dendrites of neurons expressing PEX-RFP-FKBP and KIF17-FL-GFP-FRB with (E) and without (F) HA-BICD2N-FRB.  
 (G) Percentage of neurons with retrograde and anterograde movement in proximal axon expressing the indicated constructs.  
 (H) Percentage of neurons with KIF17-FL-positive peroxisomes in dendrites expressing the indicated constructs.  
 Scale bars, 20  $\mu\text{m}$  (D), 5  $\mu\text{m}$  (E and F), and 3  $\mu\text{m}$  (B). See also [Movies S4](#) and [S5](#).

6171598). The shRNA sequences used in this study are rat KIF17 shRNA1 (5'-GCCACCAAGATTAACCTGT-3'), rat KIF17 shRNA2 (5'-GACAGGACAAAGCTCAACA-3'), rat KIF17 shRNA3 (5'-CCATCAACATCGAGATCTA-3'), and AnkyrinG shRNA (5'-GAGTTGTGCTGATGACAAG-3'). Details about the FRB/FKB constructs can be found in [11]. The following antibodies were used: rabbit-anti-KIF17 (K3638, Sigma; H-280, Santa Cruz) and mouse-anti-AnkyrinG (Invitrogen). See the [Supplemental Experimental Procedures](#).

### Cell Culture, Transfections, and Live-Cell Imaging

Primary hippocampal neurons were harvested from rat E18 embryos, cultured on poly-L-lysine (35  $\mu$ g/ml)- and laminin (5  $\mu$ g/ml)-coated coverslips in neurobasal medium (NB) supplemented with B27, 0.5 mM glutamine, 12.5  $\mu$ M glutamate, and Pen/Strep and transfected with Lipofectamine 2000 (Invitrogen). Imaging experiments were performed on Nikon Eclipse TE2000E microscope equipped with 40 $\times$  oil objective, CoolSNAP CCD camera (Photometrics), perfect-focus system, and imaging chamber. Imaging chamber was maintained at 37°C and 5% CO<sub>2</sub> during acquisition. See the [Supplemental Experimental Procedures](#).

### SUPPLEMENTAL INFORMATION

Supplemental Information includes Supplemental Experimental Procedures, three figures, and five movies and can be found with this article online at <http://dx.doi.org/10.1016/j.cub.2016.04.057>.

### AUTHOR CONTRIBUTIONS

M.A.F., M.E.d.S., and R.P.T. designed and performed the live-cell imaging experiments and analyzed the results; E.T. performed staining experiments in young neurons and analyzed the data; Y.C., C.P.F., A.F.J.J., and P.S.W. cloned constructs; L.C.K. supervised the research; and C.C.H. supervised the research, coordinated the study, and wrote the manuscript with input from all authors.

### ACKNOWLEDGMENTS

This work was supported by the Netherlands Organization for Scientific Research (NWO; NWO-ALW-VIDI, L.C.K.; NWO-ALW-VICI, C.C.H.), the Foundation for Fundamental Research on Matter (FOM; L.C.K. and C.C.H.), which is part of the NWO, the Netherlands Organization for Health Research and Development (ZonMW-TOP, C.C.H.), the European Research Council (ERC; ERC starting, L.C.K.; ERC consolidator, C.C.H.). M.E.d.S. is supported by Fundação para a Ciência e Tecnologia (FCT, Portugal; grant SFRH/BD/68642/2010), and Y.C. is part of the China Scholarship Council-Utrecht University (CSC-UU) PhD program.

Received: September 6, 2015

Revised: March 16, 2016

Accepted: April 22, 2016

Published: June 2, 2016

### REFERENCES

- Kapitein, L.C., and Hoogenraad, C.C. (2011). Which way to go? Cytoskeletal organization and polarized transport in neurons. *Mol. Cell Neurosci.* *46*, 9–20.
- Rolls, M.M. (2011). Neuronal polarity in *Drosophila*: sorting out axons and dendrites. *Dev. Neurobiol.* *71*, 419–429.
- Setou, M., Nakagawa, T., Seog, D.H., and Hirokawa, N. (2000). Kinesin superfamily motor protein KIF17 and mLin-10 in NMDA receptor-containing vesicle transport. *Science* *288*, 1796–1802.
- Guillaud, L., Setou, M., and Hirokawa, N. (2003). KIF17 dynamics and regulation of NR2B trafficking in hippocampal neurons. *J. Neurosci.* *23*, 131–140.
- Chu, P.J., Rivera, J.F., and Arnold, D.B. (2006). A role for Kif17 in transport of Kv4.2. *J. Biol. Chem.* *281*, 365–373.
- Irla, M., Saade, M., Fernandez, C., Chasson, L., Victorero, G., Dahmane, N., Chazal, G., and Nguyen, C. (2007). Neuronal distribution of spatial in the developing cerebellum and hippocampus and its somatodendritic association with the kinesin motor KIF17. *Exp. Cell Res.* *313*, 4107–4119.
- Kayadjanian, N., Lee, H.S., Piña-Crespo, J., and Heinemann, S.F. (2007). Localization of glutamate receptors to distal dendrites depends on subunit composition and the kinesin motor protein KIF17. *Mol. Cell. Neurosci.* *34*, 219–230.
- Nakata, T., and Hirokawa, N. (2003). Microtubules provide directional cues for polarized axonal transport through interaction with kinesin motor head. *J. Cell Biol.* *162*, 1045–1055.
- Song, A.H., Wang, D., Chen, G., Li, Y., Luo, J., Duan, S., and Poo, M.M. (2009). A selective filter for cytoplasmic transport at the axon initial segment. *Cell* *136*, 1148–1160.
- Huang, C.F., and Banker, G. (2012). The translocation selectivity of the kinesins that mediate neuronal organelle transport. *Traffic* *13*, 549–564.
- Kapitein, L.C., Schlager, M.A., Kuijpers, M., Wulf, P.S., van Spronsen, M., MacKintosh, F.C., and Hoogenraad, C.C. (2010). Mixed microtubules steer dynein-driven cargo transport into dendrites. *Curr. Biol.* *20*, 290–299.
- Blasius, T.L., Cai, D., Jih, G.T., Toret, C.P., and Verhey, K.J. (2007). Two binding partners cooperate to activate the molecular motor Kinesin-1. *J. Cell Biol.* *176*, 11–17.
- Hackney, D.D., and Stock, M.F. (2000). Kinesin's IAK tail domain inhibits initial microtubule-stimulated ADP release. *Nat. Cell Biol.* *2*, 257–260.
- Yamada, K.H., Hanada, T., and Chishti, A.H. (2007). The effector domain of human Dlg tumor suppressor acts as a switch that relieves autoinhibition of kinesin-3 motor GAKIN/KIF13B. *Biochemistry* *46*, 10039–10045.
- van der Vaart, B., van Riel, W.E., Doodhi, H., Kevenaer, J.T., Katrukha, E.A., Gumy, L., Bouchet, B.P., Grigoriev, I., Spangler, S.A., Yu, K.L., et al. (2013). CFEOM1-associated kinesin KIF21A is a cortical microtubule growth inhibitor. *Dev. Cell* *27*, 145–160.
- Hammond, J.W., Blasius, T.L., Soppina, V., Cai, D., and Verhey, K.J. (2010). Autoinhibition of the kinesin-2 motor KIF17 via dual intramolecular mechanisms. *J. Cell Biol.* *189*, 1013–1025.
- Coy, D.L., Hancock, W.O., Wagenbach, M., and Howard, J. (1999). Kinesin's tail domain is an inhibitory regulator of the motor domain. *Nat. Cell Biol.* *1*, 288–292.
- Imanishi, M., Endres, N.F., Gennerich, A., and Vale, R.D. (2006). Autoinhibition regulates the motility of the *C. elegans* intraflagellar transport motor OSM-3. *J. Cell Biol.* *174*, 931–937.
- Hoogenraad, C.C., Wulf, P., Schiefermeier, N., Stepanova, T., Galjart, N., Small, J.V., Grosveld, F., de Zeeuw, C.I., and Akhmanova, A. (2003). Bicaudal D induces selective dynein-mediated microtubule minus end-directed transport. *EMBO J.* *22*, 6004–6015.
- Kapitein, L.C., Schlager, M.A., van der Zwan, W.A., Wulf, P.S., Keijzer, N., and Hoogenraad, C.C. (2010). Probing intracellular motor protein activity using an inducible cargo trafficking assay. *Biophys. J.* *99*, 2143–2152.
- Soppina, V., Rai, A.K., Ramaiya, A.J., Barak, P., and Mallik, R. (2009). Tug-of-war between dissimilar teams of microtubule motors regulates transport and fission of endosomes. *Proc. Natl. Acad. Sci. USA* *106*, 19381–19386.
- Winckler, B., Forscher, P., and Mellman, I. (1999). A diffusion barrier maintains distribution of membrane proteins in polarized neurons. *Nature* *397*, 698–701.
- Al-Bassam, S., Xu, M., Wandless, T.J., and Arnold, D.B. (2012). Differential trafficking of transport vesicles contributes to the localization of dendritic proteins. *Cell Rep.* *2*, 89–100.
- Petersen, J.D., Kaech, S., and Banker, G. (2014). Selective microtubule-based transport of dendritic membrane proteins arises in concert with axon specification. *J. Neurosci.* *34*, 4135–4147.
- Baas, P.W., Deitch, J.S., Black, M.M., and Banker, G.A. (1988). Polarity orientation of microtubules in hippocampal neurons: uniformity in the axon and nonuniformity in the dendrite. *Proc. Natl. Acad. Sci. USA* *85*, 8335–8339.

26. Fu, M.M., and Holzbaur, E.L. (2014). Integrated regulation of motor-driven organelle transport by scaffolding proteins. *Trends Cell Biol.* *24*, 564–574.
27. Yin, X., Feng, X., Takei, Y., and Hirokawa, N. (2012). Regulation of NMDA receptor transport: a KIF17-cargo binding/releasing underlies synaptic plasticity and memory in vivo. *J. Neurosci.* *32*, 5486–5499.
28. Wong, R.W., Setou, M., Teng, J., Takei, Y., and Hirokawa, N. (2002). Overexpression of motor protein KIF17 enhances spatial and working memory in transgenic mice. *Proc. Natl. Acad. Sci. USA* *99*, 14500–14505.
29. Yin, X., Takei, Y., Kido, M.A., and Hirokawa, N. (2011). Molecular motor KIF17 is fundamental for memory and learning via differential support of synaptic NR2A/2B levels. *Neuron* *70*, 310–325.
30. Maeder, C.I., Shen, K., and Hoogenraad, C.C. (2014). Axon and dendritic trafficking. *Curr. Opin. Neurobiol.* *27*, 165–170.